



Optics Letters

Completely non-invasive cell manipulation in lens-integrated microfluidic devices by single-fiber optical tweezers

CHUNLEI JIANG,^{1,*†} YUNKAI WANG,^{1,†} TAIJI DONG,¹ DONG LI,¹ BING YAN,^{2,3}  PENG CHEN,¹ KEYONG SHAO,¹ XIUFANG WANG,¹ AND ZENGBO WANG^{2,4} 

¹College of Electrical and Information Engineering, Northeast Petroleum University, Daqing 163318, China

²School of Computer Science and Electronic Engineering, Bangor University, Dean Street, Bangor, Gwynedd, LL57 1UT, UK

³Center of Optics Health, Suzhou Institute of Biomedical Engineering and Technology, Chinese Academy of Sciences, No. 88 Keling Street, Suzhou Jiangsu, 215163, China

⁴zengbo.wang@gmail.com

[†]These authors contributed equally to this work.

*jiangchunlei_nepu@163.com

Received 24 January 2023; revised 7 March 2023; accepted 10 March 2023; posted 16 March 2023; published 12 April 2023

In a fiber-based optical tweezer system, it is a common practice to insert the fiber probe into the sample solution to perform the tweezer function. Such a configuration of the fiber probe may lead to unwanted contamination and/or damage to the sample system and is thus potentially invasive. Here, we propose a completely non-invasive method for cell manipulation by combining a microcapillary microfluidic device and an optical fiber tweezer. We demonstrate that *Chlorella* cells inside the microcapillary channel can be successfully trapped and manipulated by an optical fiber probe located outside of the microcapillary, thus making the process completely non-invasive. The fiber does not even invade the sample solution. To our knowledge, this is the first report of such a method. The speed of stable manipulation can reach the 7 $\mu\text{m/s}$ scale. We found that the curved walls of the microcapillaries worked like a lens, which helped to boost the light focusing and trapping efficiency. Numerical simulation of optical forces under medium settings reveals that the optical forces can be enhanced by up to 1.44 times, and the optical forces can change direction under certain conditions. © 2023 Optica Publishing Group

<https://doi.org/10.1364/OL.486264>

Single-cell analysis [1] has received increasing attention in recent years. Biological samples of interest often consist of heterogeneous cell populations. Studying heterogeneous cells is vital for drug discovery [2] and understanding basic developmental biology [3]. For example, the heterogeneity that exists in tumor cells makes them resistant to anticancer drugs, thus limiting the ability to predict the response of individual cancer patients to treatment [4].

Traditional “bulk” studies of millions of cells in a single experiment can only provide general and average results for cell behavior [5]. However, as individual cells experience and respond differently in their microbial niches, or due to the random expression of genes, special cellular properties appear

even within the same cell population [6]. There are many cell analysis methods based on different principles such as microfluidic systems [7], magnetism [8], dielectrophoresis (DEP) [9], and acoustic separation [10]. All of these techniques can be used to analyze large numbers of cells quickly and efficiently. During the manipulation process, they often affect a certain number of cells simultaneously, but it is difficult to manipulate a single cell in a population of cells.

At present, single cells are usually captured in biological experiments using holding pipettes. Negative pressure is used to aspirate single cells into holding pipettes for cell injection [4] and cellular elasticity measurement [11]. However, the mechanical force exerted on the cell membrane by this method may still lead to cell damage.

Optical tweezers [OT] [12], a flexible and widely used particle manipulation tool, can manipulate a single particle in a swarm of micron-sized particles. The combination of OT with a microfluidic chip [13] has brought great benefits to medical and biological research. However, since microfluidic chips are usually made of PDMS, it is generally necessary to use 3D optical tweezers with complex structures to complete the manipulation of particles inside the chip. 3D optical tweezers usually need to use higher laser power, and the radiation damage to cells cannot be ignored [14]. Alternatively, the optical fiber tweezers (OFT) are integrated into the microfluidic chip, which also leads to a loss of flexibility of the OFT. The particle manipulation method using OFT has the advantages of good controllability and low power. Compared with dual-fiber optic tweezers [15,16], single-fiber optical tweezers (SFOT) [17,18] have a more compact structure.

In this Letter, we present a completely non-invasive method for cell manipulation using SFOT in a microcapillary microfluidic device. To our knowledge, this is the first report of such a method. Two different single-fiber probes were used to manipulate cells at different positions in the microcapillary. The microcapillary itself has a lensing function; it works as a lens that contributes to light focusing. We calculated the enhancing

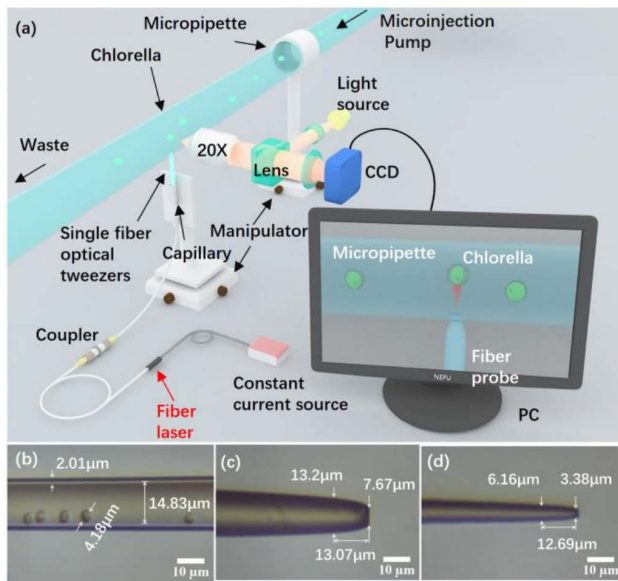


Fig. 1. (a) Schematic of the experimental setup. (b) Microcapillaries and *Chlorella* at the lower inner surfaces of microcapillaries. (c) Fiber probe with a flat fiber tip. (d) Fiber probe with a parabolic-like fiber tip.

effects of microcapillaries with different diameters (in radians) on the light force and selected the microcapillary with the most appropriate diameter for the manipulation experiment. Through this method, we can manipulate particles without touching the sample solution while maintaining the advantages of SFOT.

A schematic diagram of the experimental setup is shown in Fig. 1(a). The light source used in the experiment is a fiber laser with a wavelength of 980 nm. Most living substances have poor absorption at this wavelength [19]. The power of the laser is 25 mW.

We use flame-heated taper drawing to fabricate microcapillaries with internal diameters of 10–30 μm [Fig. 1(b)], and attach them to a glass slide with tape. The test sample is *Chlorella* cells with a diameter of 3–5 μm . We dilute the sample solution with distilled water to avoid the microcapillaries becoming clogged and the *Chlorella* adhering to the capillary surface. The microinjection pump is used to inject the *Chlorella* solution into the microcapillaries and control the flow rate. The fiber probes are made by flame heating technology using commercial single-mode fiber (G.652.D, core diameter: 9 μm). First, the fiber is wrapped in a stainless steel capillary to prevent fiber breakage and warping (outer diameter: 0.5 mm, wall thickness: 0.1 mm, length: 30 mm). Then the buffer layer and polymer sheath of the fiber are stripped with a fiber stripper, with a stripping length of 5 cm. The fiber is heated for about 30 s to reach its melting point and then stretched at an initial speed of about 2 mm/s. The fiber diameter reduces from 125 μm to 20 μm over a length of 20 mm. The stretching speed is different for fabricating fiber probes with a flat fiber tip [Fig. 1(c)] and fiber probes with a parabolic-like fiber tip [Fig. 1(d)]. The fiber tip breaks into a plane with a diameter of 7.67 μm when the stretching speed increases to 25 mm/s. The stretching speed needs to increase to 15 mm/s to fabricate the parabolic-like fiber probe. Finally, the stretching is finished by gently wiping the fiber tip with a cotton towel moistened with alcohol.

In this experiment, the size of the trapped particle is larger than the wavelength of the laser beam, which satisfies the conditions for Mie scattering. The optical forces can be divided into two components: the gradient force (F_g), which pulls particles toward areas of the highest intensity, and the scattering force (F_s), which pushes particles in the direction of the laser. The optical forces acting on the *Chlorella* can be expressed as [20]

$$\mathbf{F}_O = \oint_S \langle \langle \mathbf{T}_M \rangle \cdot \mathbf{n} \rangle dS, \quad (1)$$

where S is the closed surface surrounding the element and \mathbf{n} is the surface normal vector.

To explain and analyze the optical forces and the effect of the microcapillary lens on the laser beam, we use the wave optics module (electromagnetic waves, frequency domain) and perfectly matched layer boundary conditions in the commercial finite-element simulation software COMSOL MuTiphysics 5.6 for 2D simulation. Under an optical fiber tweezer with the same laser power, the longitudinal velocity of smaller cells is greater than the longitudinal velocity of larger cells. However, the larger particles interact more with the focused beam than the smaller cells, so, when captured, the larger cells receive stronger trapping forces [21,22]. The diameter of *Chlorella* is set to 3.6 μm . The internal diameters of the microcapillaries range from 10 to 30 μm . The wall thickness of microcapillaries is set to 0.125 times the internal radius of the microcapillaries. The position of the fiber tip is set to $x=0$, and the fiber axis is set to $y=0$. The refractive indices of air, water, and *Chlorella* cells are 1, 1.33, and 1.45, respectively, and the refractive indices of the fiber probe and microcapillaries are 1.46 [23]. The power measured at the flat fiber tip is 14.34 mW, and that at the parabolic-like fiber tip was 15.57 mW. Because the optical power of the input port in the simulation cannot actually be measured, we set the input power to 1 mW. To study the focusing effect of the microcapillary wall on optical tweezers, we use microcapillaries of different internal diameters and a glass plane of the same thickness and keep the rest unchanged in the simulation.

In Figs. 2(a) and 2(b), the internal diameter of the microcapillary is 18 μm . The distance between the fiber tip and microcapillary outer wall is set to $d_1 = 3 \mu\text{m}$. *Chlorella* is set at $x = 20 \mu\text{m}$. It is obvious that the microcapillary lens makes the diameter of the laser beam narrower when the fiber probe with a flat tip is used. Therefore, the optical forces along both the x axis and the y axis are enhanced. When we use the fiber probe with a parabolic-like tip [Figs. 2(c) and 2(d)]; the results are similar to those shown in Figs. 2(a) and 2(b). The internal diameter of the microcapillary is 18 μm . The distance between the fiber tip and microcapillary outer wall is set to $d_2 = 1.4 \mu\text{m}$. *Chlorella* is set at $x = 4.4 \mu\text{m}$. When calculating the transverse optical force, to make the calculation range wider and closer to where the actual *Chlorella* is controlled, we set the position of the *Chlorella* at $x = 18 \mu\text{m}$ and $x = 5.2 \mu\text{m}$.

Axial forces were calculated for the optical force of *Chlorella* from the bottom of the microtubule to the top of the microtubule. The longitudinal force was obtained by calculating the offset of *Chlorella* ($\pm 5 \mu\text{m}$) from the fiber tip. The cylindrical lens made of microcapillaries turns the circular Gaussian beam at the fiber tip into an ellipsoidal beam. As the number of radians gets bigger (the internal diameter gets smaller), the microcapillaries make the focus closer to the fiber tip on the x axis and closer to the fiber axis on the y axis. The best enhancing effect of both kinds

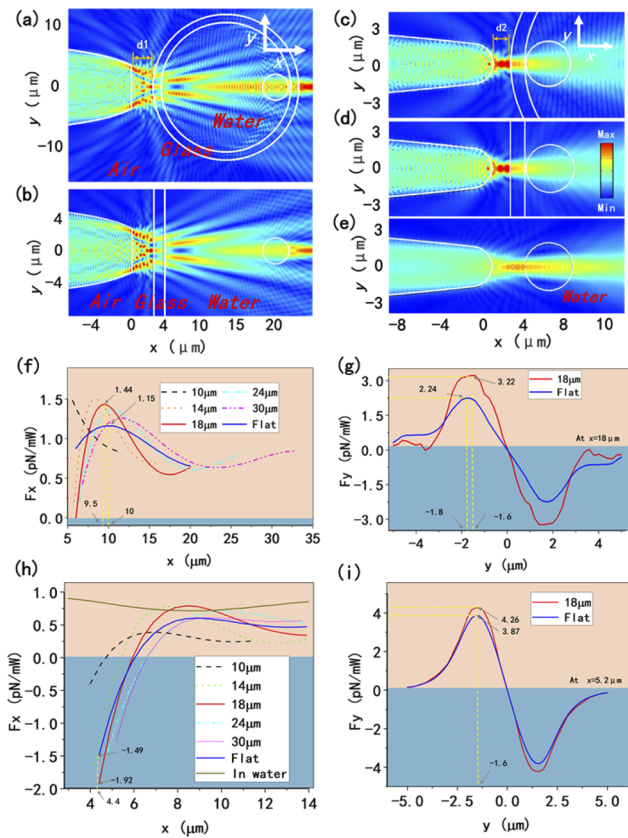


Fig. 2. Electric field intensity distribution and simulated optical forces. (a), (b) Simulated electric field intensity distribution of the laser passing through the wall of the microcapillaries (a) and a glass plate of the same thickness (b) when using a fiber probe with a flat tip. (c)–(e) Simulated electric field intensity distribution of the laser passing through the wall of microcapillaries (c), a glass plate of the same thickness (d), and water (e) with a fiber probe when using a parabolic-like tip. (f), (g) Optical forces along the x axis and y axis of *Chlorella* with a flat tip. (h), (i) Optical forces along the x axis and y axis of *Chlorella* with a flat tip and with a parabolic-like tip, respectively.

of fiber tips occurs between 14 μm and 24 μm . In Figs. 2(f) and 2(g), compared to the flat fiber tip combined with a flat glass with no radians, the optical forces are magnified by 1.25 times on the x axis and 1.44 times on the y axis when the flat fiber tip is combined with the 18- μm -internal-diameter microcapillaries. In Figs. 2(h) and 2(i), compared to the parabolic-like fiber tip combined with a flat glass with no radians, optical forces are magnified by 1.29 times on the x axis and 1.1 times on the y axis when the parabolic-like fiber tip is combined with the 18- μm -internal-diameter microcapillaries. We also calculated the electric field intensity distribution of the parabolic optical tweezers in water [Fig. 2(e)]. It is worth mentioning that the optical force direction of the parabolic-like tip in water is opposite to that of the parabolic-like tip–microcapillary structure, as proved in our experiments [Fig. 2(h)].

To experimentally verify non-contact particle manipulation with the SFOT, we use SFOT with different optical force directions (pull or push) to control the movement of *Chlorella* in the microcapillaries. The diameter of the microcapillaries ranges from 14 to 24 μm , which is the best result of the simulation. We first demonstrate the pushing operation with flat fiber tips,

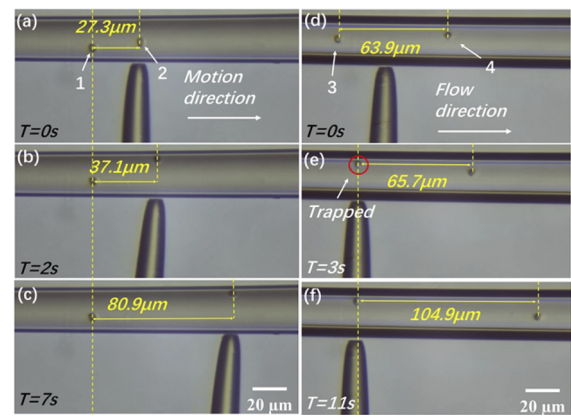


Fig. 3. Manipulating cells on the upper inner surface of microcapillaries using SFOT with a flat fiber tip.

as shown in Figs. 3(a)–3(c). The sample solution is still. Here, *Chlorella* cell no. 1 in the figure is not affected by optical forces and is used for reference. Particle no. 2 is the manipulated *Chlorella* cell. The F_s pushes the *Chlorella* cell against gravity to the upper inner surface of the microcapillaries. When moving the fiber probe, the *Chlorella* deviates from the area with maximum optical intensity. The F_g helps to drag it right in front of the fiber probe. The maximum moving speed of cell manipulation laterally is 7.7 $\mu\text{m/s}$.

In Figs. 3(d)–3(f), *Chlorella* cells are propelled by microfluidics. They move to the right at a speed of 4.9 $\mu\text{m/s}$ within the microcapillaries [Fig. 3(d)]. We use a fiber probe with a flat tip to fix *Chlorella* cells. Particle no. 3 is the reference *Chlorella* cell propelled by microfluidics, and particle no. 4 is the *Chlorella* cell to be fixed. *Chlorella* is stably trapped at the upper inner surface of the microcapillaries [Figs. 3(e) and 3(f)].

Furthermore, as shown in Figs. 4(a)–4(c), the sample solution is static. We use SFOT with a parabola-like fiber tip for the pulling operation. This keeps the *Chlorella* on the lower inner surface of microcapillaries. *Chlorella* cell no. 5 is not affected by the optical forces and is used for reference. Particle no. 6 is the *Chlorella* cell that is manipulated. The *Chlorella* can be manipulated laterally at the lower inner surface of microcapillaries. The manipulation speed is 7.1 $\mu\text{m/s}$. In Figs. 4(d)–4(f), we test the direction of the optical force when the fiber probe and *Chlorella* are both in water without microcapillaries. Particle no. 7 is the reference that is not affected by the optical forces. Particle no. 8 is the *Chlorella* cell that is manipulated. The results show that *Chlorella* is pushed away from the fiber probe.

In our experiment, microcapillaries with an internal diameter of about 18 μm are used as the microfluidic carrier; they have a shape similar to those of capillaries in the living body. The microcapillary wall functions as a lens that focuses light. Due to astigmatism, the focal length is closer to the fiber tip longitudinally and laterally. Because the refractive index of air is lower than that of water, the deflection angle of the laser exiting the fiber is greater, and the arc of microcapillary lens brings the focus closer to the fiber tip. It is worth mentioning that the F_g and F_s of the optical tweezers did not reach a balance, and the *Chlorella* was pressed onto the microtubule wall by the pulling or pushing to achieve a force balance. We also calculated the forces in the z -direction of *Chlorella* using a simplified 3D model, and the results were similar to those in the y -direction.

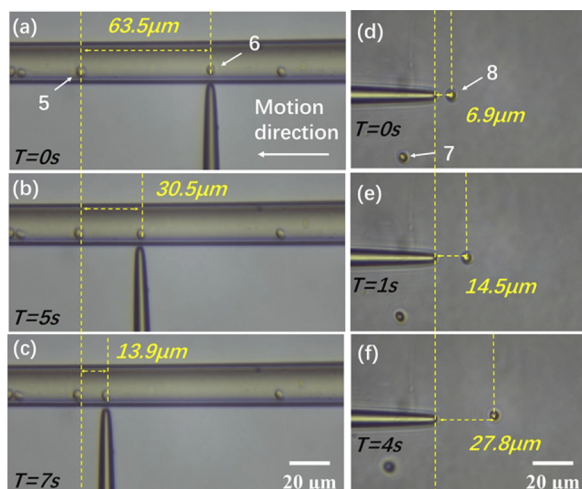


Fig. 4. (a)–(c) Manipulating cells on the lower inner surface of microcapillaries using SFOT with a parabola-like fiber tip. (d)–(f) Manipulating cells in solution using SFOT with a parabola-like fiber tip. See also [Visualization 1](#), [Visualization 2](#), [Visualization 3](#), and [Visualization 4](#).

In summary, we have presented a completely non-invasive method for cell manipulation using SFOT in a microcapillary-lens-integrated microfluidic device. We use microcapillaries with an internal diameter of about $18\ \mu\text{m}$ as a microfluidic carrier. To our knowledge, this is the first report of the use of SFOT to manipulate *Chlorella* in microcapillaries. The method not only isolates the sample and the fiber probe but also focuses the laser. The optical fiber is set in the vertical direction, which improves the efficiency of the optical capture. It's easy to capture the cells that sink to the bottom. This method maintains the advantages of SFOT, such as good controllability, low power, and a compact structure, and reduces contamination and damage. It provides new possibilities for particle transport, the capture of rare cells, and the study of cell-to-cell interactions.

Funding. Natural Science Foundation of Heilongjiang Province (LH2021F008).

Disclosures. The authors declare no conflicts of interest.

Data availability. Data underlying the results presented in this paper are not publicly available at this time but may be obtained from the authors upon reasonable request.

REFERENCES

1. L. X. Liu, D. Y. Chen, J. B. Wang, and J. Chen, *Cells* **9**, 1271 (2020).
2. A. M. Ghaemmaghami, M. J. Hancock, H. Harrington, H. Kaji, and A. Khademhosseini, *Drug Discovery Today* **17**, 173 (2012).
3. D. S. Adams and M. Levin, *Cell Tissue Res.* **352**, 95 (2013).
4. S. Ma, P. Wang, W. H. Zhou, D. P. Chu, S. K. Zhao, L. Fu, and Y. Li, *Theriogenology* **141**, 142 (2020).
5. A. Keloth, O. Anderson, D. Risbridger, and L. Paterson, *Micromachines* **9**, 434 (2018).
6. D. Di Carlo and L. P. Lee, *Anal. Chem.* **78**, 7918 (2006).
7. J. S. Kwon and J. H. Oh, *Appl. Sci.* **8**, 992 (2018).
8. M. Z. Yang, X. Y. Wu, H. L. Li, G. C. Cui, Z. Y. Bai, L. Wang, M. Kraft, G. Z. Liu, and L. G. Wen, *J. Micromech. Microeng.* **31**, 034003 (2021).
9. P. R. Zhang, L. H. Ren, X. Zhang, Y. F. Shan, Y. Wang, Y. T. Ji, H. B. Yin, W. E. Huang, J. Xu, and B. Ma, *Anal. Chem.* **87**, 2282 (2015).
10. M. A. Faridi, H. Ramachandraiah, I. Iranmanesh, D. Grishenkov, M. Wiklund, and A. Russom, *Biomed. Microdevices* **19**, 23 (2017).
11. Y. W. Liu, M. S. Cui, J. J. Huang, M. Z. Sun, X. Zhao, and Q. Zhao, *Micromachines* **10**, 348 (2019).
12. A. Ashkin, *Phys. Rev. Lett.* **24**, 156 (1970).
13. C. Faigle, F. Lautenschlager, G. Whyte, P. Homewood, E. Martin-Badosa, and J. Guck, *Lab Chip* **15**, 1267 (2015).
14. M. A. S. de Oliveira, D. S. Moura, A. Fontes, and R. E. de Araujo, *J. Biomed. Opt.* **21**, 075012 (2016).
15. Y. Li, X. Liu, X. Xu, H. Xin, Y. Zhang, and B. Li, *Adv. Funct. Mater.* **29**, 1905568 (2019).
16. A. Asadollahbaik, A. Kumar, M. Heymann, H. Giessen, and J. Fick, *Opt. Lett.* **47**, 170 (2022).
17. S. Liu, Z. Li, Z. Weng, Y. Li, L. Shui, Z. Jiao, Y. Chen, A. Luo, X. Xing, and S. He, *Opt. Lett.* **44**, 1868 (2019).
18. Y. X. Zhang, C. Wang, Y. Zhang, X. Y. Tang, Y. Zhou, Z. H. Liu, J. Z. Zhang, and L. B. Yuan, *J. Lightwave Technol.* **40**, 1144 (2022).
19. F. M. Fazal and S. M. Block, *Nat. Photonics* **5**, 318 (2011).
20. X. Zhao, N. Zhao, Y. Shi, H. Xin, and B. Li, *Micromachines* **11**, 114 (2020).
21. Y. C. Li, H. B. Xin, C. Cheng, Y. Zhang, and B. J. Li, *Nanophotonics* **4**, 353 (2015).
22. J. E. Melzer and E. McLeod, *ACS Nano* **12**, 2440 (2018).
23. H. B. Xin, Y. C. Li, and B. J. Li, *Adv. Funct. Mater.* **25**, 2816 (2015).